Title	Two-directional N2 desorption in thermal dissociation of N2O on Rh(110), Ir(110), and Pd(110) at low temperatures
Author(s)	Horino, H.; Rzez'nicka, I.; Kokalj, A. et al.
Citation	Journal of Vacuum Science & Technology A: Vacuum, Surfaces, and Films, 20(5), 1592-1596 https://doi.org/10.1116/1.1495507
Issue Date	2002-09
Doc URL	https://hdl.handle.net/2115/5733
Type	journal article
File Information	JVS&TA-VSF20(5).pdf

Two-directional N$_2$ desorption in thermal dissociation of N$_2$O on Rh(110), Ir(110), and Pd(110) at low temperatures

H. Horino and I. Rzeźnicka
Department of Materials Science, Graduate School of Environmental Earth Science, Hokkaido University, Sapporo 060-0810, Japan

A. Kokalj and I. Kobal
J. Stefan Institute, 1000 Ljubljana, Slovenia

Y. Ohno, A. Hiratsuka, and T. Matsushima[a)]
Surface Reaction Dynamics Laboratory, Catalysis Research Center, Hokkaido University, Sapporo 060-0811, Japan

Two-directional N$_2$ desorption was found in N$_2$O dissociation on Rh(110), Ir(110), and Pd(110) below 160 K by angle-resolved thermal desorption. N$_2$O(a) is mostly dissociated during heating procedures, emitting N$_2$(g) and leaving O(a). N$_2$ showed four desorption peaks in the temperature range of 110–200 K. One of them commonly showed a cosine distribution, whereas the others sharply collimated off the surface normal in the plane along the [001] direction. The collimation angle was about 70° on Rh(110), 65° on Ir(110), and 43°–50° on Pd(110). A high-energy-atom assisted desorption model was proposed for N$_2$ inclined emission. © *2002 American Vacuum Society.* [DOI: 10.1116/1.1495507]

I. INTRODUCTION

N$_2$O decomposition on noble metals has attracted much attention in the catalytic removal of nitrogen oxides in exhaust gases because these metals are good catalysts and N$_2$O is the main by-product in this process.[1] Furthermore, N$_2$O itself is harmful and yields a remarkable greenhouse effect. However, its decomposition and formation mechanism on these metals is not clear. Peculiar N$_2$ desorption observed on Pd(110) is expected to provide more insight into product emission dynamics.[2–6] This paper is the first to report the angular distributions of desorbing N$_2$ in the thermal dissociation of N$_2$O(a) on Rh(110) and Ir(110) as well as Pd(110). Part of the desorbing N$_2$ commonly collimated far from the surface normal in the plane along the [001] direction. The collimation angle changed significantly according to the metal that was used.

We recently found a close similarity in the angular and velocity distributions of desorbing N$_2$ in both NO and N$_2$O decompositions over Pd(110) (Refs. 2–6) and concluded that a substantial contribution to N$_2$ emission originated from the N$_2$O(a) intermediate in a steady-state NO+CO reaction. Desorbing N$_2$ with a hyperthermal energy was highly concentrated in the plane along the [001] direction and collimated at 41°–43° off the surface-normal. The inclined emission was explained to be due to decomposition of N$_2$O(a) molecules oriented along the [001] direction, in which a nascent oxygen atom could provide a surface parallel momentum to desorbing N$_2$.[2,3] Such oriented N$_2$O has recently been confirmed to be stable by a density functional theory (DFT) study.[7] This high-energy-atom assisted desorption model predicts larger collimation angles and higher kinetic energy on rhodium and iridium than on palladium because larger amounts of energy are released in the metal–O bond formation.[8]

II. EXPERIMENTS

An UHV system with three chambers was used.[9] The reaction chamber was equipped with LEED-AES, an Ar$^+$ gun, and a mass spectrometer for angle-integrated (AI) desorption analysis. The collimator house had a slit on each end and the analyzer had another mass spectrometer for angle-resolved (AR)-TDS measurements. A sample crystal was set on the top of a rotatable manipulator to change the desorption angle (θ; polar angle). This angle was scanned in the normally directed plane along the [001] direction because the inclined desorption was found in this plane.[5]

The sample crystal was cleaned by repeated Ar$^+$ bombardments and heating in oxygen. After being flashed to high temperatures, the surface was exposed to ^{15}N$_2$O through a gas doser when the surface temperature (T_S) was down to around 95 K. The flashing temperature was 1200 K on Rh(110) and 1000 K on Pd(110). After this flashing, the surface showed a sharp (1×1) LEED pattern without higher-order spots. No reactive oxygen remained, as judged from the absence of CO$_2$ formation in the post-TDS after CO exposure. The LEED pattern still showed (1×1) on Rh(110) after TDS work of N$_2$O below about 200 K. On the other hand, an Ir(110) surface was first heated in 3×10^{-8} Torr O$_2$ for 900 s at T_S=870 K and then in 3×10^{-8} Torr H$_2$ for 600 s at T_S=500 K. It was finally heated to 1100 K in vacuum. The resultant surface was partially reconstructed into a missing-row structure.[10] It was exposed to H$_2$ at 0.3 L (Langmuir) and flashed to 1100 K before each experiment.

The fragmentation of ^{15}N$_2$O was separately examined in

each mass spectrometer under a constant flow of this gas. The correction based on this fragmentation became significant only at high exposures. Hereafter, the isotope ^{15}N is simply designated as N.

III. RESULTS

After N_2O exposures at 95 K or below it, $N_2O(a)$ mostly dissociated in the subsequent heating procedures common to the three surfaces, emitting $N_2(g)$ and leaving $O(a)$. N_2 showed four desorption peaks in the temperature range of 110–200 K. On the other hand, N_2O desorption was noticed only above exposures yielding near saturation of N_2 desorption on Rh(110) and Pd(110). On Rh(110), N_2O desorption peaked at around 115 K and was completed at around 130 K. Its peak area in the AI-form was always below 10% of that of N_2. On Pd(110), the peak area was <1% of that of N_2 and its desorption was completed at around 150 K. On the other hand, on Ir(110), N_2O desorption was noticed above one third of saturation of N_2 and its peak area reached about 30% of that of N_2. Thus, the N_2O coverage, Θ_{N_2O}, was defined as the AI-TDS peak area of N_2 relative to the maximum, commonly on the three surfaces.

A. Rh(110)

N_2 desorption started at around 95 K and two peaks first appeared at 110 K (β_4-N_2) and 167 K (β_1-N_2) when the clean surface was exposed to N_2O at 95 K. Significant signals were observed between the above two peaks, suggesting the presence of additional peaks [Fig. 1(a)]. The β_4-N_2 signal was enhanced in the AR form around $\theta = 70°$ as compared with that in the AI form. For the angular distribution analysis, the peak temperature and peak height of each N_2 desorption were determined by curve fitting, in which a Gaussian form with fixed values for its peak position and half-width was assumed for each peak (Fig. 1). The remaining signal, after subtraction of β_1-N_2 and β_4-N_2, seemed to involve two peaks at around 130 K and 145 K, and the signal is called (β_2-$N_2 + \beta_3$-N_2). This component was highly enhanced at high exposures and overlapped with the others. The formation of β_1-N_2 at around 167 K was major from low exposures and showed a simple cosine distribution [Fig. 2(a)]. The signal of β_4-N_2 was maximized at $\pm 70°$ and approximated as $\cos^{15}(\theta + 70) + \cos^{15}(\theta - 70)$ [Fig. 2(b)]. The (β_2-$N_2 + \beta_3$-N_2) signal followed a similar angle dependence to β_4-N_2.

We also examined the angular distribution of desorbing N_2 from the clean surface exposed to N_2 at 95 K. N_2 desorption in the subsequent heating peaked at 165 K below two thirds of saturation. This showed a simple cosine distribution. Hence, a β_1-N_2 peak was assigned to the desorption from an adsorption state as $N_2(a)$.

B. Ir(110)

After N_2O exposure, N_2 desorbed in the temperature range from 100 K to 210 K (Fig. 3). The main peaks were found at 120 K (β_4-N_2) and 190 K (β_1-N_2). The signal between them was still significant and involved (β_2-N_2
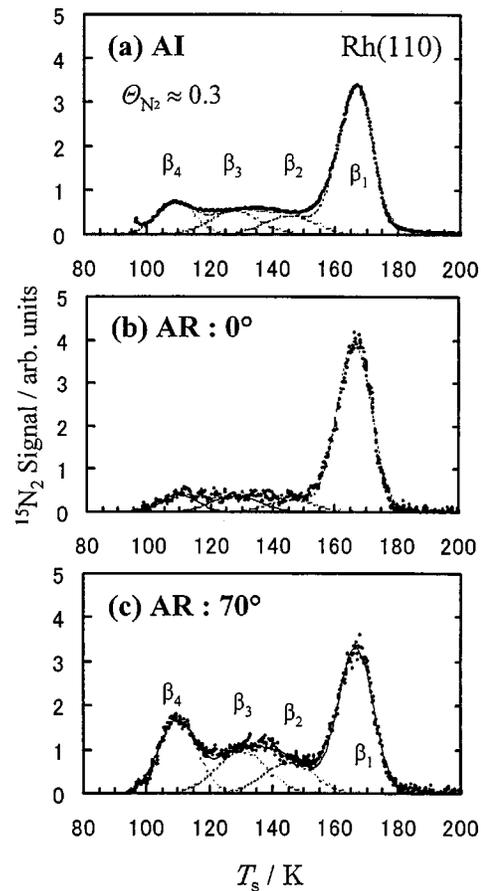
FIG. 1. TDS spectra of N_2 from N_2O-covered Rh(110) at $\Theta_{N_2O} = 0.3$. (a) AI-form, (b and c) AR-form at $\theta = 0°$ and 70°. The heating rate was 0.6 K s^{-1}. Deconvolutions shown by dotted curves are based on a Gaussian form for each peak. The solid line indicates the sum of all the components.

$+ \beta_3$-N_2) at around 145 K and 168 K. It was insensitive to the desorption angle. β_1-N_2 showed a simple cosine distribution and the peak temperature was very close to the N_2 desorption peak position on clean Ir(110). This is due to desorption from a molecularly adsorbed state of N_2. β_4-N_2 showed inclined desorption that collimated at $65 \pm 5°$ and was accompanied with a cosine distribution component (Fig. 4). The signal was approximated as $\cos^{15}(\theta + 65) + \cos^{15}(\theta - 65) + 0.6 \cos \theta$.

C. Pd(110)

N_2 desorption showed four peaks in a temperature range of 100–160 K. The AR-TDS spectra were sensitive to the desorption angle, as shown in Fig. 5. β_4-N_2 was clearly seen only at $\Theta_{N_2O} < 0.10$ in the AR form at around $\theta = 35° - 65°$ and peaked at 110 K.[11] The β_3-N_2 peak was sharply enhanced above $\Theta_{N_2O} = 0.05$ at 123 K. β_1-N_2 appeared at around 150 K as a shoulder of intense β_2-N_2, becoming evident at high N_2O exposures. With increasing Θ_{N_2O}, β_2-N_2 increased linearly. Its formation peaked at around 134 K and was always major. This component was insensitive to θ, showing a cosine distribution, and its peak temperature
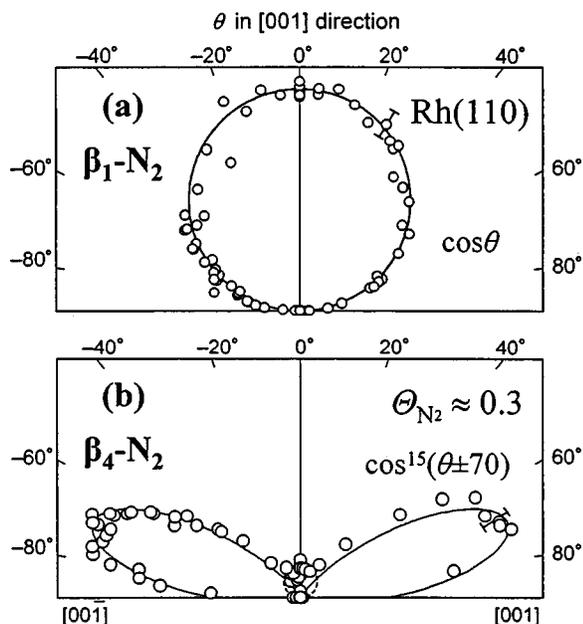
θ in [001] direction

FIG. 2. Angular distributions of desorbing N$_2$ in the plane along the [001] direction on Rh(110). (a) β_1-N$_2$ at $T_S = 167$ K and $\Theta_{N_2O} = 0.3$. (b) β_4-N$_2$ at $T_S = 110$ K and $\Theta_{N_2O} = 0.3$. Error bars are also shown.
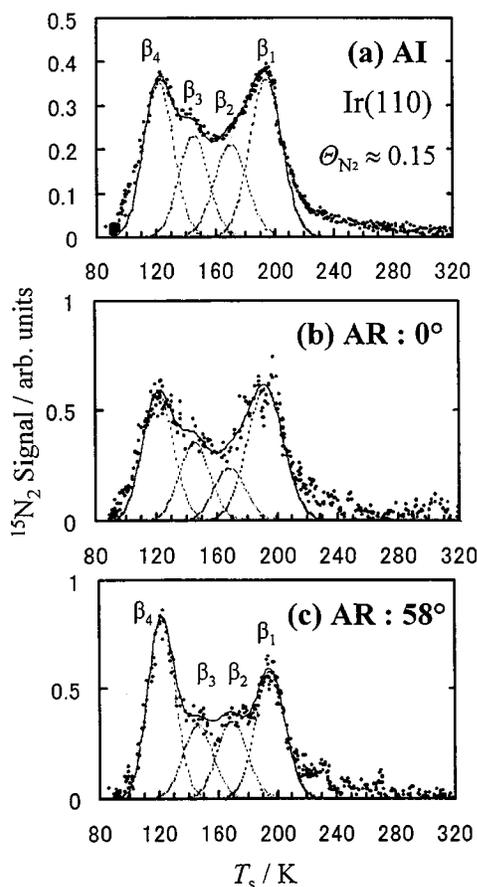

θ in [001] direction

FIG. 4. Angular distribution of β_4-N$_2$ in the plane along the [001] direction on Ir(110) at $T_S = 120$ K and $\Theta_{N_2O} = 0.15$. A typical error level is shown by the inclined bar.

agreed with the desorption of N$_2(a)$ on clean Pd(110). This is again due to the desorption from a molecular N$_2$ adsorption state.

The angular distributions of the other three components are summarized in Fig. 5(c). β_4-N$_2$ obeyed a $\cos^{28}(\theta+50) + \cos^{28}(\theta-50)$ form at $\Theta_{N_2O} < 0.10$. The collimation angle shifted from 50° to 44° above $\Theta_{N_2O} = 0.20$ and showed a $\cos^{50}(\theta+44) + \cos^{50}(\theta-44)$ form. β_3-N$_2$ collimated at $\pm43°$. Its signal was approximated as $\cos^{50}(\theta+43) + \cos^{50}(\theta-43)$. β_1-N$_2$ obeyed a $\cos^{50}(\theta+43) + \cos^{50}(\theta-43)$ form. These powers have experimental uncertainty as 50 ± 10.

The N$_2$ TDS shape changed depending on the precoverage of oxygen. No N$_2$ was desorbed when the surface was covered in advance with oxygen to more than one-third of saturation. With increasing the preadsorbed oxygen, β_4-N$_2$ and β_3-N$_2$ were suppressed quickly, whereas β_2-N$_2$ was once maximized at around 10% of saturation of oxygen and then decreased.

IV. DISCUSSION

A. Diffuse distribution

N$_2$O decomposition yielded four N$_2$ desorption peaks in the range of 110–200 K. One of them commonly showed a cosine distribution. On Pd(110), the velocity of N$_2$ in this peak was already analyzed to show a Maxwellian distribution at the surface temperature.[6] This is consistent with desorption from the adsorption state of N$_2$. Such N$_2(a)$ formation may proceed below their peak temperatures as N$_2$O(a) → N$_2(a)$ + O(a). The peak temperature is simply determined by the heat of N$_2$ adsorption.

This cosine component contributed about 50% of the total amount of desorbing N$_2$ on Pd(110) at low N$_2$O exposures, whereas on Rh(110), it was about 70%. On Ir(110), it was roughly 80% when considering that β_4-N$_2$ involved a cosine component to about 30% and the others were in a cosine distribution. From the desorption peak temperature, the heat of adsorption of N$_2$ was estimated to be about 34 kJ mol^{-1} on Pd(110), 42 kJ mol^{-1} on Rh(110), and 38–48 kJ mol^{-1} on Ir(110).[12] This order is fairly consistent with the fraction se-

FIG. 3. TDS spectra of N$_2$ from N$_2$O-covered Ir(110) at $\Theta_{N_2O} = 0.15$. (a) AI-form, and (b and c) AR-form at $\theta = 0°$ and $\theta = 58°$. The heating rate was 3 K s^{-1}. Deconvolutions shown by dotted curves are based on a Gaussian form for each peak. The solid line indicates the sum of all the components.
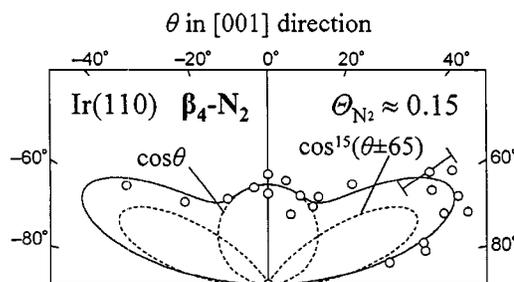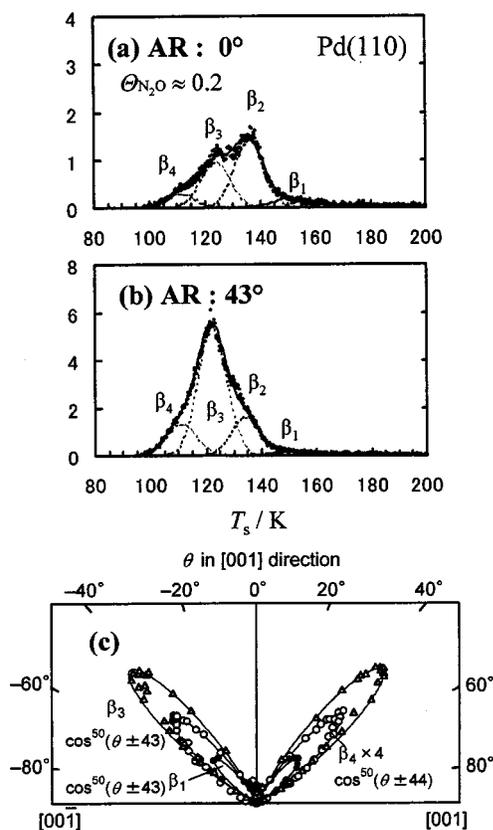
FIG. 5. AR-TDS spectra of N_2 at different desorption angles from N_2O-covered Pd(110) at $\Theta_{N_2O}=0.20$. (a) $\theta=0°$ and (b) $\theta=43°$. The heating rate was 0.6 K s^{-1}. Deconvolutions shown by dotted curves are based on a Gaussian form for each peak. The solid line indicates the sum of all the components. (c) Angular distribution of each N_2 peak in the plane along the [001] direction. ●, β_1-N_2 at $T_S=150$ K and $\Theta_{N_2O}=1.0$, and at $\Theta_{N_2O}=0.20$; △, β_3-N_2 at $T_S=123$ K and ○, β_4-N_2 at $T_S=110$ K.

quence of the cosine component, suggesting that a principal factor to control the trapping is the depth of the N_2 adsorption potential well.

The other N_2 peaks are due to direct desorption from the $N_2O(a)$ decomposition events because of their sharp angular distributions. The differences in the peak temperature are due to the different activation energies of $N_2O(a)$ decomposition. This energy may increase with increasing the amount of $O(a)$ because of the decreasing vacant sites and the stabilizing effect toward the $N_2O(a)$.[13]

B. Inclined desorption

β_1-N_2 on Pd(110) carries a hyperthermal energy (about 46 kJ mol^{-1}).[2–5] N_2 in the other inclined desorption is also expected to show high translational energy because of its sharp angular distributions.[14] The collimation angle depends on the kind of metal, i.e., $70°\pm5°$ on Rh(110), $65°\pm5°$ on Ir(110), and $43°–50°$ on Pd(110). This sequence is consistent with our prediction described in the introduction.

The bent N_2O molecule oriented into the [001] direction is suitable for the precursor of dissociation because it interacts with metal also through its terminal oxygen atom which must be removed by the surface.[7] After the N–O bond is

broken, the nascent $O(a)$ is stabilized onto the nearest adsorption site. During this process, a large amount of energy is dissipated on account of the energy of the metal–O bond formation. The released energy on Pd(110) is ≈200 kJ mol^{-1} since the heat of N_2O adsorption is only 25–35 kJ mol^{-1} and the heat of the Pd–O formation is about 235 kJ mol^{-1}.[8,11] Therefore, the fragment N_2 is able to receive energy from the nascent O atom.

The released energy is much higher on Rh and Ir. It was estimated to be ≈350 kJ mol^{-1} because the heat of the metal–O bond formation is around 374 kJ mol^{-1} for Rh and 378 kJ mol^{-1} for Ir.[8] Hence, the experimentally observed trend in the collimation angle can be explained because it is reasonable to assume that the larger the dissipated energy release from the metal–O bond formation and the associated force is presumably acting along the [001] direction on the remaining N_2 fragment, the more the collimation angle will shift from the [110] surface normal direction.

The energy transfer mechanism is not clear at present. The nascent N_2 may be repelled by the surface along the surface normal due to Pauli repulsion because the bulky N_2 molecule is formed in a close proximity to the surface. Such repulsion was reported in the combinative desorption as $2N(a) \rightarrow N_2(g)$ on Ru(001) and Cu(111).[15–17] The force is exerted to the product along the surface normal because normally directed desorption was observed. However, the normally directed force in N_2O dissociation is not expected to be as large as that in the combinative desorption because the location of N in $N_2O(a)$ is further from the surface than that of the adsorbed nitrogen atom. For inclined desorption, additional forces must be operative towards the product N_2 into the inclined way. This force is likely to come from the nascent oxygen.

A higher translational energy is generally expected for molecules with sharper angular distributions,[18] although the translational energy generally depends on the surface crystal azimuth.[14] The above model predicts that the translational energy on Rh(110) and Ir(110) is higher than that on Pd(110), i.e., the angular distribution on Pd(110) must be broader than that on the others. However, the sharpness of the angular distribution was observed in an opposite way. This discrepancy must be directly examined by velocity distribution measurements.

V. SUMMARY

The angular distribution of desorbing N_2 in N_2O dissociation on Rh(110), Ir(110), and Pd(110) was analyzed by angle-resolved thermal desorption. The results are summarized as follows:

(1) N_2 showed four desorption peaks in the range of 110–200 K. One of the peaks commonly shows a cosine distribution due to desorption from $N_2(a)$.
(2) N_2 desorbing in the other peaks sharply collimates off the surface normal into the [001] direction. The collimation angle was about $70°$ on Rh(110), $65°$ on Ir(110), and $43°–50°$ on Pd(110).

ACKNOWLEDGMENTS

[1] V. I. Pǎrvulescu, P. Grange, and B. Delmon, Catal. Today **46**, 233 (1998).
[2] Y. Ohno, K. Kimura, M. Bi, and T. Matsushima, J. Chem. Phys. **110**, 8221 (1999).
[3] I. Kobal, K. Kimura, Y. Ohno, and T. Matsushima, Surf. Sci. **445**, 472 (2000).
[4] I. Kobal, K. Kimura, Y. Ohno, H. Horino, I. Rzeźnicka, and T. Matsushima, Stud. Surf. Sci. Catal. **130**, 1337 (2000).
[5] I. Rzeźnicka, Y. Ohno, I. Kobal, H. Horino, K. Kimura, and T. Matsushima, in *Heterogeneous Catalysis*, in Proceedings of the 9th International Symposium, edited by L. Petrov, Ch. Bonev, and G. Kadinov, 2000, p. 97 (unpublished).
[6] Y. Ohno, I. Kobal, H. Horino, I. Rzeźnicka, and T. Matsushima, Appl. Surf. Sci. **169/170**, 273 (2001).
[7] A. Kokalj, I. Kobal, H. Horino, Y. Ohno, and T. Matsushima, Surf. Sci. **506**, 196 (2002).
[8] D. L. Hildenbrand and K. H. Lau, Chem. Phys. Lett. **319**, 95 (2000).
[9] T. Matsushima, Surf. Sci. **127**, 403 (1983).
[10] T. Matsushima, Y. Ohno, and K. Nagai, J. Chem. Phys. **94**, 704 (1991).
[11] H. Horino, S. Liu, A. Hiratsuka, Y. Ohno, and T. Matsushima, Chem. Phys. Lett. **341**, 419 (2001).
[12] D. E. Ibbotson, T. S. Wittrig, and W. H. Weinberg, Surf. Sci. **110**, 313 (1981).
[13] H. H. Huang, C. S. Seet, Z. Zou, and G. Q. Xu, Surf. Sci. **356**, 181 (1996).
[14] T. Matsushima, Heterog. Chem. Rev. **2**, 51 (1995).
[15] T. Matsushima, Surf. Sci. **197**, 287 (1988).
[16] M. J. Murphy, J. F. Skelly, and A. Hodgson, J. Chem. Phys. **109**, 3619 (1998).
[17] M. J. Murphy, J. F. Skelly, A. Hodgson, and B. Hammer, J. Chem. Phys. **110**, 6954 (1999).
[18] G. Comsa and R. David, Surf. Sci. Rep. **5**, 145 (1985).